

# Application of the Rotating Cylinder Electrode—E-Brite<sup>(1)</sup> 26-1/Concentrated Sulfuric Acid\*

D. C. SILVERMAN and M. E. ZERR\*

## Abstract

The corrosion of E-Brite 26-1 has been examined in concentrated sulfuric acid (70 to 93 wt%) using the rotating cylinder electrode (RCE). Two stable corrosion potentials were found: (1) in the passive voltage region and (2) in the active voltage region. Only the active potential is stable after the alloy is cathodically polarized. The corrosion rate at this potential is controlled by the rate of mass transfer of  $\text{FeSO}_4$  from a saturated surface salt film to the bulk fluid. Enhanced mass transfer caused by surface roughening was detected. The corrosion rate calculated from the active anodic current density (CD) limit obtained from polarization scans agrees with that calculated from weight loss. Practical and rapid velocity testing is possible using only the polarization scans generated from the RCE.

## Introduction

Concentrated sulfuric acid (>70 wt%) is a highly corrosive, yet industrially important commodity chemical. The specification of appropriate materials of construction for containment of this acid is an ongoing problem. Mass transfer-controlled corrosion is one of the mechanisms by which some iron-base alloys degrade in this environment. The rate-controlling step for such a mechanism is usually considered to be the rate of mass transfer of iron ions from a saturated layer of  $\text{FeSO}_4$  on the alloy surface. This mechanism has been demonstrated for the corrosion of carbon steel in concentrated sulfuric acid.<sup>1,2</sup> If corrosion is under mass transfer control, fluid velocity-sensitive corrosion would be expected to occur in any plant equipment made from an alloy exhibiting such sensitivity.

This discussion suggests that fluid motion under defined hydrodynamic conditions should be included in a materials evaluation involving concentrated sulfuric acid. Two primary laboratory techniques are available for evaluating mass transfer-controlled corrosion, pipe loops, and rotating electrodes. As discussed previously, pipe loops tend to be cumbersome to operate and require copious amounts of fluid.<sup>3</sup> Thus, the rotating electrode is probably the best practical system for evaluating the possibility of mass transfer-controlled corrosion in concentrated sulfuric acid.

One question that arises is how such an effect might be evaluated quickly and easily. As shown by Ellison and Schmeal,<sup>1</sup> the current obtained by controlling the potential of iron in 68 wt%  $\text{H}_2\text{SO}_4$  in the region of the anodic current limit could be used to calculate Sherwood numbers that obey the mass transfer-Reynolds number relationship for a rotating cylinder electrode (RCE). This effect has been demonstrated for carbon steel in 93 wt%  $\text{H}_2\text{SO}_4$ .<sup>4</sup> These results suggest that

<sup>(1)</sup>Registered trade name.

\* Presented during CORROSION/86, Paper No. 268, Houston, Texas.

\* Monsanto Co., 800 N. Lindbergh Blvd., St. Louis, Missouri 63167.

a rapid electrochemical test to determine whether mass transfer affects the corrosion in concentrated sulfuric acid might be feasible. The test would use the maximum current density (CD) just cathodic to the primary passivation potential as measured on a polarization scan to evaluate mass transfer control. If mass transfer controls the corrosion rate, this CD should at least approximate the anodic CD limit or the mass transfer rate. Thus, velocity sensitivity might be evaluated rapidly without waiting either to obtain a weight loss or to monitor a current at the anodic current limit for extended time periods.

The anodic CD limit as estimated from a polarization scan has been used to examine the performance of E-Brite 26-1 in concentrated sulfuric acid, especially in the 93 wt% range. Although the study of iron-chromium alloys is extensive, no data have been reported on the performance of these alloys in concentrated sulfuric acid. However, the available results do suggest that a velocity sensitivity might be expected. These results tend to be for dilute sulfuric acid and sulfate solutions in the pH range of 0 to 2.

El-Basiouny and Haruyama<sup>5</sup> examined the polarization behavior of six iron-chromium alloys in sulfate solutions. The polarization scans for alloys containing 5 to ~12 wt% chromium revealed that the alloy dissolution is similar to that of pure iron. Thus, at least for lower chromium concentrations, iron-chromium alloys and iron might behave similarly in sulfuric acid.<sup>6,7</sup> Molybdenum additions have been shown to affect the critical CD at voltages just cathodic to the passivation voltage.<sup>8</sup> This finding suggests that the presence of molybdenum might affect alloy performance in concentrated sulfuric acid.

The possibility of a mass transfer influence on the corrosion of iron-chromium alloys in dilute (1 M)  $\text{H}_2\text{SO}_4$  has been examined using the rotating disk electrode (RDE).<sup>9</sup> The chromium content of the alloys studied was in the range of 10 to 22 wt%. Mass transfer was found to affect the corrosion of all of these alloys. Although two parallel dissolution processes are suggested by the data, at least one of these pathways seems to depend on mass transfer. No statement was made concerning the species that cause the mass transfer limitation.

However, the surface and solution characterization results of Leygraf, et al.<sup>10</sup> on iron-chromium-molybdenum alloys suggest that the mass transfer-limiting species is either Fe<sup>+2</sup> or an iron-containing salt. Selective dissolution of iron was detected in these latter studies.

These results imply that the possibility of a mass transfer-influenced corrosion mechanism must be considered during an evaluation of E-Brite 26-1 in concentrated sulfuric acid. Therefore, the RCE was used for the study to maintain controlled hydrodynamics under conditions that might best simulate those found in the plant.<sup>3</sup> The anodic CD limit was used as estimated both from a polarization scan and from weight loss to evaluate the influence of mass transfer on corrosion.

## Experimental

### Apparatus

The experimental setup was discussed in detail previously.<sup>3</sup> An outer cylinder was formed by the Pyrex<sup>(2)</sup> wall of the cylindrical vessel. A platinum screen counter electrode 7.5-cm high by 7.5-cm diameter rested against the inside wall of the vessel. The top was a tightly fitting Teflon<sup>(3)</sup> block. Thus, all of the experiments must be considered to be under air saturation, the conditions found in the plant for the system under study.

The working inner cylinder electrode had an inner Hastelloy<sup>(4)</sup> G shaft that connected to the rotator. A hollow Teflon sleeve isolated the inner shaft from the outer working electrode. The outer portion was composed of four parts: (1) an upper Hastelloy G sleeve, against which the silver-carbon brush of the rotator rested; (2) a Rulon<sup>(5)</sup> spacer; (3) the working sample; and (4) another Rulon spacer. The entire assembly was held together by a Hastelloy G end bolt. When operating, the liquid interface was kept at about the midpoint of the upper Rulon spacer to help eliminate end effects. The end of the Luggin-Haber capillary was kept as close as possible to the interface between the upper Rulon spacer and working electrode.

The rotator used was an ASR2 Analytical Rotator manufactured by Pine Instruments, Inc.,<sup>(6)</sup> which has a variable speed control from 20 to 10,000 rpm. A PAR<sup>(7)</sup> 173D potentiostat with a 376 logarithmic converter was used to vary the potential relative to a remote reference electrode, and a PAR 175 Universal Programmer was used to scan voltages. The temperature was controlled by a Model 51 automatic temperature controller manufactured by Love Control Corp.<sup>(8)</sup> For this study, the reference electrode was a saturated mercury-mercurous sulfate reference electrode from Radiometer America, Inc.<sup>(9)</sup>

### Materials

Two types of sulfuric acid were used for the study. One batch of 93 wt% sulfuric acid was industrial grade. This acid contained ~44 ppm iron impurity by weight, as measured by inductively coupled argon plasma (ICAP). All of the other acid concentrations (70 to 93 wt%) were diluted from Fisher<sup>(10)</sup> ACS reagent grade sulfuric acid using deionized water. The strength of the final diluted acid was analyzed and was always within ~0.5 wt% of the desired concentration.

The E-Brite 26-1 was commercial grade; its compositions are given in Table 1. One heat was used for the experiments in the industrial grade (93 wt% H<sub>2</sub>SO<sub>4</sub>), and the other was used for the reagent grade acid. The compositions are similar, and

(2)-(5) Registered trade names.

(6) Pine Instruments, Inc., Grove City, Pennsylvania.

(7) EG & G Princeton Applied Research, Princeton, New Jersey.

(8) Love Control Corp., Wheeling, Illinois.

(9) Radiometer America, Inc., Westlake, Ohio.

(10) Fisher Controls International, Inc., Marshalltown, Iowa.

TABLE 1 — Composition of E-Brite 26-1 (wt%)

Cr	Mo	Ni	Nb	Ti	C	Test
25.16	0.84	0.05	0.08	<0.01	<0.01	93 wt% (industrial)
25.75	0.99	0.15	0.14	<0.01	<0.01	Other acid concentrations

both heats were exposed to acid of comparable strength. This use of different heats is not expected to affect the results.

### Procedure

Before the polarization scans were generated, the electrode was immersed in the sulfuric acid at the desired rotation rate, and the voltage was monitored until a stable corrosion potential was established. Several hours were sometimes required to achieve a stable corrosion potential. The potential was anodically increased at 0.5 mV·s<sup>-1</sup> (1.8 V·h<sup>-1</sup>) until ~10<sup>4</sup> mA·m<sup>-2</sup> was reached. Then the scan was reversed, and the voltage was ramped back through the corrosion potential. The initial corrosion potential was sometimes in the passive region of the curve [0.0 to 0.2 V (Hg-Hg<sub>2</sub>SO<sub>4</sub>)]. If so, the same anodic scan was generated, but the cathodic portion was continued until the active portion of the curve was passed. This active portion usually occurred at -0.8 to -0.9 V (Hg-Hg<sub>2</sub>SO<sub>4</sub>). Then the corrosion potential was allowed to reestablish itself, and the anodic polarization scan was repeated. This second corrosion potential remained in the active region. Temperatures of 303 to 373 K were used. No attempt was made to correct for the voltage drop between the Luggin-Haber capillary tip and the alloy sample.

Weight loss experiments were also run on the RCE for 24 h under controlled velocity conditions using the 80 wt% and industrial grade 93 wt% acid concentrations. The corrosion potential was monitored for the entire period. Samples of the solution were removed after ~0.5, 1, 4 to 5, and 24 h. The solutions were analyzed by ICAP for iron, chromium, and molybdenum. Temperatures of 303 to 373 K were also used for these experiments.

### Data Reduction Theory

The procedure for determining whether the mass transfer rate controls the corrosion mechanism is to compare the mass transfer coefficient calculated from the weight loss or an appropriate CD to the mass transfer coefficient expected for the experimental geometry. This procedure has been detailed elsewhere<sup>1-3</sup> and is reviewed only briefly here. The mass transfer coefficient is related to a concentration driving force between the surface and the bulk by

$$k = \frac{R}{C_S - C_B} \quad (1)$$

All of the symbols are defined at the end of this paper. Thus, if the mass transfer rate is known or can be calculated and the concentration driving force is known, the mass transfer coefficient can be calculated. The Sherwood number is calculated from this mass transfer coefficient. This Sherwood number is compared to that expected for the apparatus geometry. For the smooth rotating cylinder within a cylinder electrode, the relationship is<sup>11</sup>

$$Sh = 0.0791Re^{0.7}Sc^{0.356} \quad (2)$$

The Sherwood number can be estimated from the current

**TABLE 2 — Corrosion Potential as a Function of Temperature and Rotation Rate (93 wt% Industrial H<sub>2</sub>SO<sub>4</sub>)**

Temperature (K)	Rotation Rate (rad·s <sup>-1</sup> )	Corrosion Potential [V (Hg-Hg <sub>2</sub> SO <sub>4</sub> )]
303	0	+0.010
	5.24 × 10	+0.018
	2.09 × 10 <sup>2</sup>	+0.020
333	0	-0.771
	2.09 × 10	-0.836
	5.24 × 10	-0.844
	2.09 × 10 <sup>2</sup>	-0.870
373	0	-0.780
	2.09 × 10	-0.805
	5.24 × 10	-0.850
	1.05 × 10 <sup>2</sup>	-0.862
	2.09 × 10 <sup>2</sup>	-0.897

weight loss by

$$Sh = \left(\frac{W}{t}\right) \left(\frac{1}{A}\right) \left(\frac{1}{M}\right) \left(\frac{1}{C_S - C_B}\right) \left(\frac{d}{D}\right) \quad (4)$$

Equation (4) uses a time-averaged concentration driving force to estimate the Sherwood number. The reason for following this approach is that the bulk concentration of the rate-limiting species changes with time. The time-averaged bulk concentration can be estimated by curve fitting the measured concentration with respect to time and then dividing by the total time. The Sherwood number estimated by this procedure should agree with that calculated from Equation (2) if the corrosion rate is under mass transfer control. If the anodic CD peak can be used to estimate the mass transfer-controlled corrosion rate, the Sherwood number estimated from Equation (3) should agree with that estimated from Equation (2).

## Results

### Industrial Grade 93 wt% H<sub>2</sub>SO<sub>4</sub>

Table 2 gives the corrosion potentials for the 93 wt% sulfuric acid experiments. No periodic cycling of the corrosion potential was detected. As shown, the corrosion potentials measured at 303 K are far more positive than those measured at 333 and 373 K. Figure 1 shows an overlay of the polarization scans generated for E-Brite 26-1 at 333 K in 93 wt% H<sub>2</sub>SO<sub>4</sub>. The corrosion potentials at 303 K definitely lie in the passive region of the polarization scan, noble to what appears to be the primary passivation potential. Those measured at 333 and 373 K lie in the active region of the polarization scan, e.g., active with respect to the primary passivation potential. A distinct CD limit independent of potential occurs between ~ -0.90 and ~ -0.60 V (Hg-Hg<sub>2</sub>SO<sub>4</sub>). The primary passivation potential is virtually independent of the rotation rate. The corrosion

at the anodic peak (at the anodic CD limit) by

$$Sh = \left(\frac{i}{nF}\right) \left(\frac{1}{C_S - C_B}\right) \left(\frac{d}{D}\right) \quad (3)$$

The bulk concentration is assumed to be the impurity level of the rate-limiting ion. For this system, the rate-limiting ion is assumed to be Fe<sup>+2</sup>. The saturated surface compound is assumed to be FeSO<sub>4</sub>.

The Sherwood number can also be estimated from the

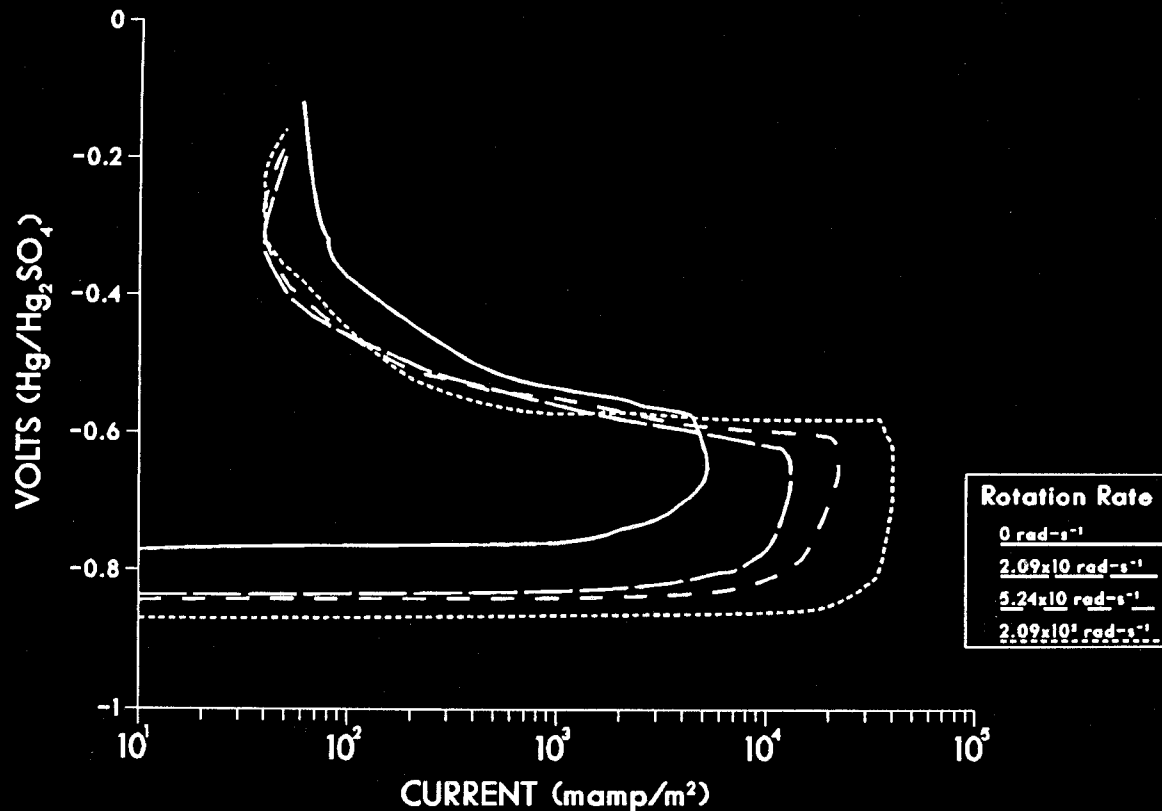


FIGURE 1 — Polarization scans of E-Brite 26-1 in industrial 93 wt% H<sub>2</sub>SO<sub>4</sub> at 333 K as a function of rotation rate.

**TABLE 3 — Corrosion Potential in Industrial 93 wt% H<sub>2</sub>SO<sub>4</sub> as a Function of Increasing Temperature**

Rotation Rate (rad·s <sup>-1</sup> )	Temperature (K)	Corrosion Potential [V (Hg-Hg <sub>2</sub> SO <sub>4</sub> )]
0	303	-0.120
	318	-0.070
	333	-0.860
0 <sup>(1)</sup>	303	-0.120
	318	-0.880
	333	-0.890
2.09 × 10	303	-0.030
	318	-0.920
	333	-0.920

<sup>(1)</sup>Repeat experiment.

potential becomes more active with increasing rotation rate. These characteristics suggest mass transfer-influenced corrosion.

The polarization scans generated at 303 K were cathodically driven through the active anodic potential region (-0.9 V ≤ voltage ≤ -0.65 V) and into the cathodic potential region. The corrosion potentials at 303 K reestablished themselves in the lower active region after removal of the applied voltage. The potentials did not return to the original values, at least during the several hours of monitoring.

In addition, the alloy potential was monitored as a function of temperature between 303 and 333 K for increasing temperature. The results are shown for 0 and 2.90 × 10 rad·s<sup>-1</sup> (0 and 200 rpm) in Table 3. Note that these potentials are not true steady-state corrosion potentials because the open circuit potential (OCP) was allowed to establish itself for only ~1 h between jumps in temperature.

#### Dilute Reagent Grade H<sub>2</sub>SO<sub>4</sub>

Polarization scans were generated for dilute reagent grade 70, 75, 80, 90, and 93 wt% H<sub>2</sub>SO<sub>4</sub>. Most of the experiments were run at 0 and 2.09 × 10<sup>2</sup> rad·s<sup>-1</sup> (0 and 2000 rpm). Table 4 gives the steady-state corrosion potentials as a function of sulfuric acid concentration, temperature, and rotation rate. The corrosion potentials labeled *after activation* were recorded after completion of the cathodic portion of the polarization scans listed immediately above them and after allowing for the potentials to reach steady state. Polarization scans were generated from this new steady-state potential. The corrosion potential did not oscillate between passive and active values. The results suggest that the recorded passive potentials were easily upset and reached values characteristic of an active type of corrosion. The polarization scans generated from these active potentials were very similar to those shown in Figure 1 for 93 wt% industrial grade H<sub>2</sub>SO<sub>4</sub>.

The corrosion potential was monitored as a function of temperature in 80 wt% H<sub>2</sub>SO<sub>4</sub> at 0 and 2.09 × 10<sup>2</sup> rad·s<sup>-1</sup>. Temperatures were increased in ~15 K increments between 303 and 373 K; then they were decreased in the same manner. After approximately each 15 K temperature change, the potential was allowed to stabilize for ~1 h. Figure 2 shows a plot of this *corrosion potential* vs the inverse of temperature. Note that between 303 and ~350 K, the potentials are virtually independent of temperature. Above 350 K, there is a slight dependence on temperature, an increase with temperature at 0 rad·s<sup>-1</sup>, and a decrease with temperature at 2.09 × 10<sup>2</sup> rad·s<sup>-1</sup>. Also note that the rotation rate causes a much stronger effect than temperature on the potential. This strong

**TABLE 4 — Steady-State Corrosion Potential as a Function of H<sub>2</sub>SO<sub>4</sub> Concentration, Temperature, and Rotation Rate**

H <sub>2</sub> SO <sub>4</sub> Concentration (wt%)	Temperature (K)	Rotation Rate (rad·s <sup>-1</sup> )	Corrosion Potential [V (Hg-Hg <sub>2</sub> SO <sub>4</sub> )]		
70 <sup>(1)</sup>	303	0	+0.144		
		2.09 × 10 <sup>2</sup>	+0.177		
	(After activation) <sup>(2)</sup>	303	2.09 × 10 <sup>2</sup>	-0.875	
			0	-0.907	
	333	0	0	-0.873	
			2.09 × 10 <sup>2</sup>	+0.067	
		(After activation) <sup>(2)</sup>	333	2.09 × 10 <sup>2</sup>	+0.123
				2.09 × 10 <sup>2</sup>	-0.887
		(After activation) <sup>(2)</sup>	373	2.09 × 10 <sup>2</sup>	+0.100
				2.09 × 10 <sup>2</sup>	-0.913
75 <sup>(1)</sup>	303	2.09 × 10 <sup>2</sup>	-0.870		
		2.09 × 10 <sup>2</sup>	-0.136		
	(After activation) <sup>(2)</sup>	333	2.09 × 10 <sup>2</sup>	-0.866	
			2.09 × 10 <sup>2</sup>	-0.874	
	(No activation)	333	2.09 × 10 <sup>2</sup>	-0.874	
			373	2.09 × 10 <sup>2</sup>	-0.960
	80 <sup>(1)</sup>	333	2.09 × 10	-0.813	
			5.24 × 10	-0.830	
			2.09 × 10 <sup>2</sup>	-0.870	
	90 <sup>(1)</sup>	333	2.09 × 10 <sup>2</sup>	-0.878	
(Repeat)			2.09 × 10 <sup>2</sup>	+0.066	
(After activation) <sup>(2)</sup>			333	2.09 × 10 <sup>2</sup>	-0.882
93 <sup>(1)</sup>	303	2.09 × 10 <sup>2</sup>	-0.813		
		(Repeat)	303	2.09 × 10 <sup>2</sup>	-0.365
	373	0	-0.818		
		2.09 × 10 <sup>2</sup>	-0.876		

<sup>(1)</sup>Reagent grade.

<sup>(2)</sup>The experiments labeled *after activation* were run following the preceding experiment and after reestablishing the steady-state corrosion potential.

effect of rotation rate on corrosion again suggests velocity-sensitive corrosion.

#### Mass Transfer Correlation

The average weight loss and maximum anodic CD at the anodic peak on the polarization scans were used to estimate the Sherwood number as a function of Reynolds number. The results for the weight loss alone are shown in Figure 3, and the combined data are shown in Figure 4. Mass transfer of FeSO<sub>4</sub> is assumed to be the rate-controlling process for this calculation. The Eisenberg, et al. correlation<sup>11</sup> is included for comparison. The line labeled *regression* is discussed later. The polarization results are calculated from the CD limit measured after the corrosion potential established itself in the active region.

The estimation of physical properties must be mentioned since reasonable estimates are critical to the results. The analysis requires estimates of the diffusion coefficient and saturation concentration of FeSO<sub>4</sub> and the density and viscosity of sulfuric acid, all as a function of acid concentration and temperature. The FeSO<sub>4</sub> saturation concentration was estimated from Silcock.<sup>12</sup> The solubility data are reported as a function of both acid concentration and temperature. A correlation was obtained between the FeSO<sub>4</sub> saturation and sulfuric acid concentrations at each temperature for sulfuric acid concentrations between 70 and 93 wt%. Different correlations were required above and below the maximum in the iron sulfate solubility, which occurs at ~85 wt% H<sub>2</sub>SO<sub>4</sub>.<sup>12</sup> The solubility-temperature curve was then established from these correlations for each sulfuric acid concentration used. The estimated saturation concentration of FeSO<sub>4</sub> in 93 wt% H<sub>2</sub>SO<sub>4</sub> agreed within ~10% with the FeSO<sub>4</sub> concentration measured after several days of rotation at 2.09 × 10<sup>2</sup> rad·s<sup>-1</sup> (2000 rpm) in 93 wt% H<sub>2</sub>SO<sub>4</sub>, at which time no change of FeSO<sub>4</sub> concentration occurred with rotation time.

The diffusion coefficient of FeSO<sub>4</sub> in H<sub>2</sub>SO<sub>4</sub> was calculated from the Wilke-type extrapolation formula<sup>13</sup> as pro-

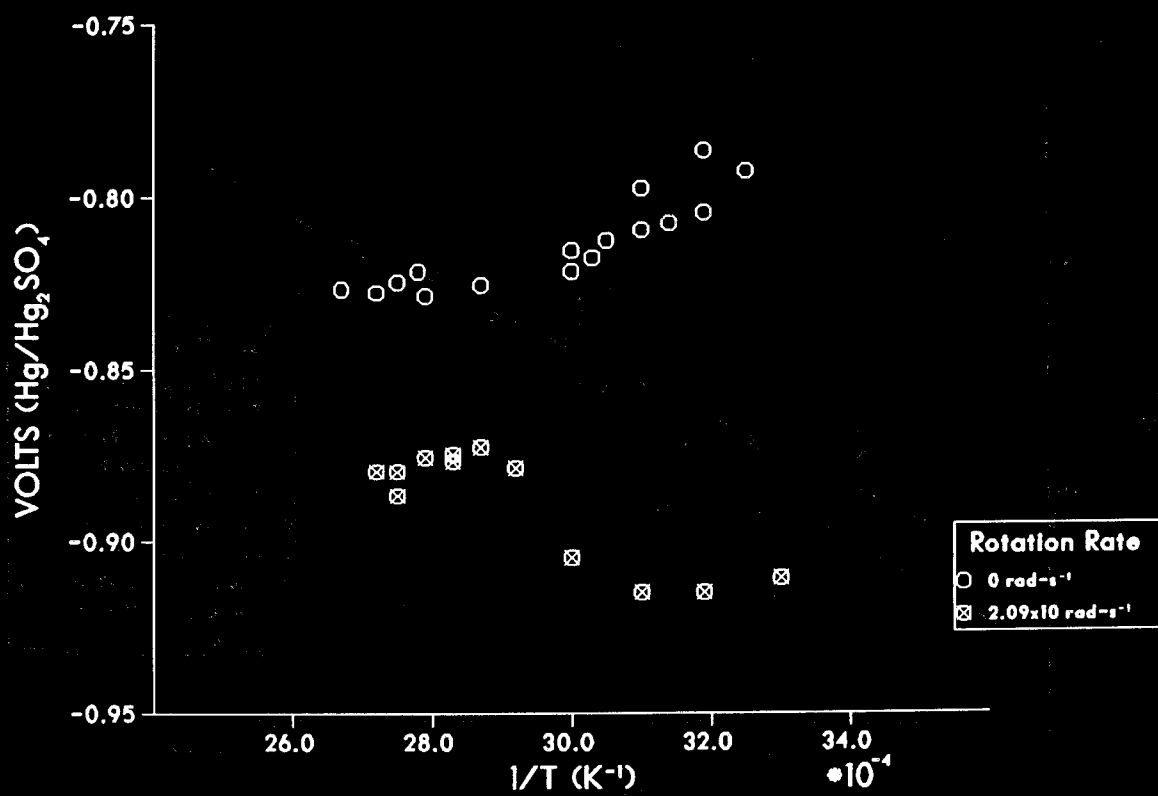


FIGURE 2 — Corrosion potential of E-Brite 26-1 in 80 wt% H<sub>2</sub>SO<sub>4</sub> as a function of temperature.

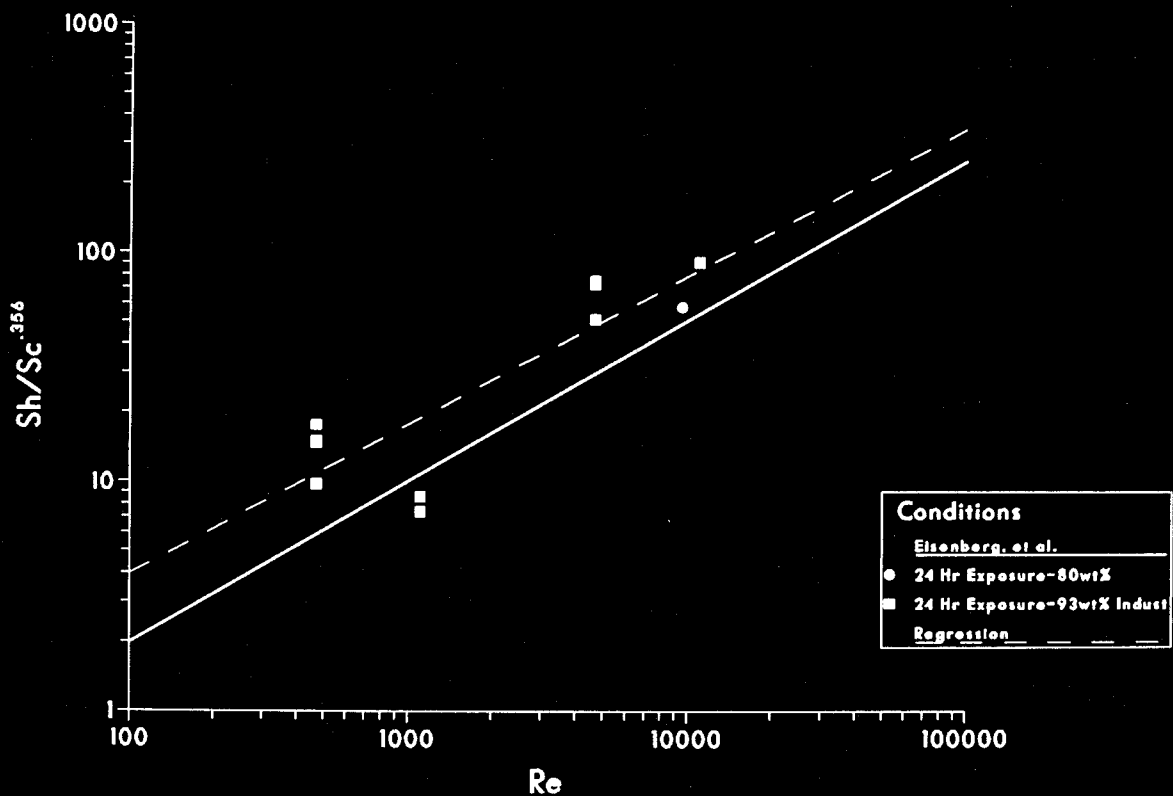


FIGURE 3 — Sherwood number-Reynolds number relationship for E-Brite 26-1 from the weight loss compared to the Eisenberg, et al., correlation<sup>11</sup> [Equation (2)].

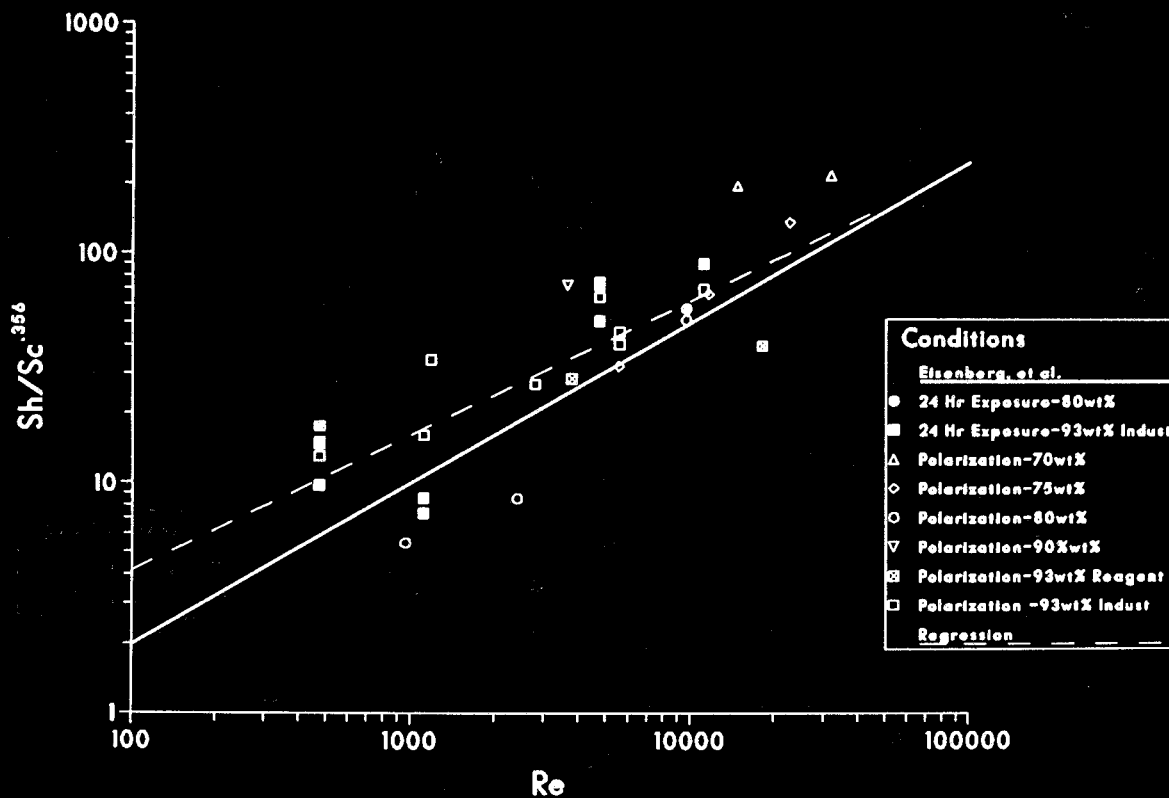


FIGURE 4 — Sherwood number-Reynolds number relationship for E-Brite 26-1 from both the weight loss and anodic CD limit compared to the Eisenberg, et al., correlation<sup>11</sup> [Equation (2)].

posed by Ellison and Schmeal<sup>1</sup> and Dean and Grab.<sup>2</sup> The equation is

$$D = 1.68 \times 10^{-14} T/\mu \quad (5)$$

The sulfuric acid viscosity data were obtained from the tabulation of Fasulo.<sup>14</sup> The sulfuric acid density data were obtained from the International Critical Tables.<sup>15</sup>

The range of Reynolds numbers covered in these experiments is  $\sim 4.5 \times 10^2 < Re < 4.0 \times 10^4$ . This range lies in the turbulent regime for the RCE.<sup>16</sup> The range of Schmidt numbers covered is  $\sim 3.5 \times 10^3 < Sc < 3.7 \times 10^5$ . This range coincides approximately with the  $10^3 < Sc < 10^5$  range for which Equation (2) is believed to describe mass transfer in the smooth RCE.<sup>11</sup> Thus, the inclusion of Equation (2) in Figures 3 and 4 is valid.

### Discussion

Figures 3 and 4 show that  $FeSO_4$  mass transfer dominates the corrosion mechanism of E-Brite 26-1 in 70 to 93 wt% concentrated sulfuric acid if the corrosion potential stabilizes in the active dissolution region. The mechanism is unchanged in both reagent grade sulfuric acid and industrial grade sulfuric acid. This mechanism is unrelated to the  $FeSO_4$  solubility maximum that occurs at  $\sim 85$  wt% sulfuric acid. The corrosion rate in this active dissolution region is controlled by the mass transfer rate of  $FeSO_4$  similar to that of carbon steel.<sup>1,2,4</sup>

A skewing of the data occurs above the correlation. This skewing might be explained by errors in the physical property estimates, especially the diffusion coefficient of  $FeSO_4$ . Until this diffusion coefficient is accurately measured, the use of Equation (5) as an estimating procedure must suffice.

Surface roughness is another possible cause of this tendency of the data to lie above the correlation for a smooth cylinder. Makanjuola and Gabe studied the enhancement of mass transfer caused by well-characterized roughness on the

rotating cylinder surface.<sup>17</sup> These authors found that surface roughness shifted the correlation to higher Sherwood numbers and larger mass transfer coefficients. The data could be correlated by an equation in which the limiting current mass transfer coefficient is proportional to either the friction velocity or the rotation rate raised to a power lying between 0.51 and 0.58. The friction velocity was proposed to be the variable for  $8 \times 10^3 < Re < 10^4$ , and the rotation rate or peripheral velocity was proposed to be the variable for  $10^4 < Re < 10^5$ .

Figures 3 and 4 show lines labeled *regression*. These lines were derived directly from the data; they have slopes of 0.65 in Figure 3 and 0.59 in Figure 4 over the range of  $4.0 \times 10^2 < Re < 2.0 \times 10^4$ . Both lines lie above the correlation for a smooth cylinder. This qualitative agreement with the results of Mankanjuola and Gabe suggests that enhanced mass transfer caused by surface roughness could explain the skewing of the data to higher values of the Sherwood number. A more quantitative comparison cannot be made since the roughness geometry of the corroding E-Brite 26-1 cylinders was different from that used by Mankanjuola and Gabe.

There seems to be no difference in alloy behavior whether exposed to the reagent or industrial grade of 93 wt% sulfuric acid. The corrosion potential in 93 wt%  $H_2SO_4$  at 333 to 373 K always seems to lie between  $-0.80$  and  $-0.90$  V (Hg- $Hg_2SO_4$ ), independent of acid origin. However, the corrosion potential established after initial immersion in lower concentrations of reagent grade acid tends to have as great a chance of lying in the active voltage region as in the passive voltage region of the potential-current relationship. This phenomenon seems to be independent of temperature and rotation rate. Thus, lower acid concentrations can lead to two possible steady-state corrosion potentials. However, in all cases, if the alloy was polarized cathodic to the lower corrosion potential, the final corrosion potential remained in that region when potential control was ended. An anodic CD limit was found when anodically polarizing the electrode from this reestablished corrosion potential.

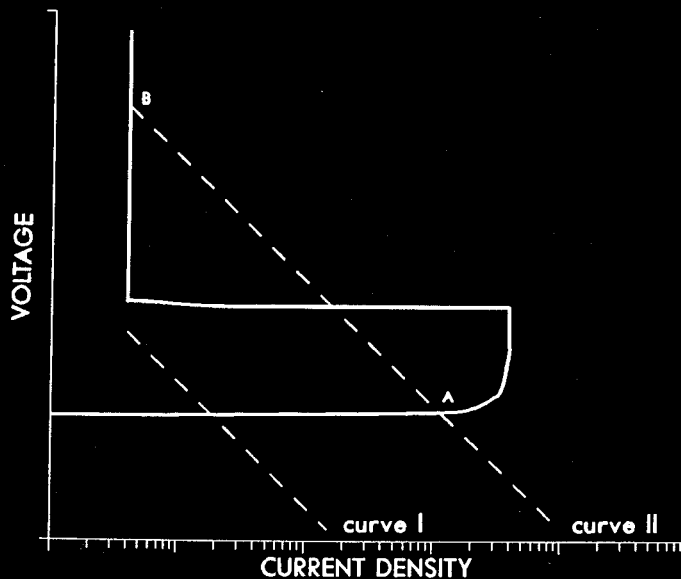


FIGURE 5 — Idealized anodic and cathodic polarization scans of E-Brite 26-1 in concentrated sulfuric acid (see text for details).

This phenomenon can be explained by the schematic polarization diagram shown in Figure 5, in which idealized anodic and cathodic curves are overlaid. The behavior of E-Brite 26-1 in 93 wt% sulfuric acid (reagent or industrial grade) above  $\sim 333$  K suggests that the polarization curve is best represented by the sum of the cathodic Curve 1 and the anodic curve. There is only one intersection of these curves. Thus, there is only one stable corrosion potential, as was observed.

The behavior in 93 wt%  $H_2SO_4$  below  $\sim 333$  K and in the lower acid concentrations is best depicted by the intersection of cathodic Curve 2 and the anodic curve. Two stable intersection points exist (A and B). Thus, both points could be observed in the laboratory, even under the same conditions of temperature and acid concentration, depending on factors such as surface condition, alloy constituents in the surface region, etc. However, activation of the E-Brite 26-1 to potentials cathodic to Point A seems to disrupt the passive surface film. Concentrated sulfuric acid does not allow the surface to repair itself rapidly, and the corrosion potential remains at Point A.

The corrosion potential in the passive region at Point B on Figure 5 is probably created by oxygen present in the bulk solution. A current limit was observed when cathodically polarizing from this corrosion potential. Such a current limit, which occurred at voltages below  $\sim -0.2$  V (Hg-Hg<sub>2</sub>SO<sub>4</sub>), could have been caused by oxygen mass transfer. No such current limit was observed when cathodically polarizing from the corrosion potential that was established in the active region (Point A in Figure 5).

A hypothesis might be made that the passivity at Point B is established by chromium oxide<sup>10,18</sup> or possibly an iron-chromium oxide with an enrichment of chromium.<sup>19</sup> Upon cathodically polarizing the alloy or even by simply immersing it in concentrated sulfuric acid, passivity is lost as accelerated iron dissolution disrupts the passive film. The alloy then behaves like carbon steel, as if the chromium and molybdenum are not present. Possible reasons for these phenomena are that (1) the surface concentration of chromium may have decreased or (2) the structure of the chromium oxide may have changed so that chromium oxide no longer creates a corrosion barrier. Note that iron chromite and hydrated chromium oxide are slightly soluble in acidic solution.<sup>20</sup> Possibly, the external environment can alter the surface composition. The resulting increase in iron dissolution may actually prevent the chromium oxide film

from healing itself. Thus, iron dissolution continues virtually unhindered. This mechanism is supported by the rotating disk results for iron-chromium alloys in 1 M  $H_2SO_4$ . One of the corrosion pathways has been hypothesized to be a velocity-sensitive dissolution of iron even in the presence of chromium on the alloy surface.<sup>9</sup> Obviously, surface characterization is necessary to monitor changes in the alloy surface composition and electronic interactions as a function of polarization and sulfuric acid concentration. The practical significance of this study is that E-Brite 26-1 should not be used in this range of sulfuric acid concentrations. Passivity, if it is observed, is not stable passivity and might be easily lost.

The agreement between the Sherwood numbers calculated by the different procedures (weight loss vs anodic CD peak on the polarization scan) suggests that the estimated anodic CD limit could be used to assess whether a velocity sensitivity is present and whether such a sensitivity is caused by mass transfer control. Increased scatter seems to occur in the Sherwood numbers calculated from the polarization scans. This increased scatter could be caused by the polarization-based anodic CD limit not being the actual steady-state limit. A slower scan rate may have been required to more closely approximate steady state. The scatter is most notable for the 70 wt% acid strength. The reason is unclear. Thus, use of the current limit on the polarization scan yields only an estimated current limit. However, the estimate is reliable enough to be used to demonstrate velocity sensitivity and possibly even mass transfer control.

Thus, all that is required to make a practical assessment of mass transfer control using the RCE is a series of polarization scans run at several different rotation rates. If mass transfer affects the anodic reaction, curves similar to those in Figure 1 would be found. If mass transfer affects the cathodic reaction (for example, oxygen mass transfer), a current limit in the cathodic region would be found.<sup>21</sup> Either current limit would increase with the rotation rate. The practical implication of this finding is that the RCE could be used fairly rapidly to determine whether mass transfer can influence or control the corrosion rate. Of course, the rate-limiting species would have to be either known or guessed, and physical property data would have to be known or estimated to use the RCE quantitatively.

## Conclusions

1. Use of the RCE has revealed that E-Brite 26-1 can exhibit two corrosion potentials in concentrated sulfuric acid (70 to 93 wt%) containing oxygen. Only the active corrosion potential is stable, especially after cathodic polarization.
2. The corrosion rate at the active corrosion potential is controlled by the mass transfer rate of FeSO<sub>4</sub> from a saturated surface salt film. The alloy behaves in a manner analogous to mild steel.
3. The RCE is a practical tool for predicting velocity-sensitive corrosion. Rapid testing is possible using the polarization scans generated with this tool.

## References

1. B. T. Ellison, W. R. Schmeal, *J. Electrochem. Soc.*, Vol. 125, No. 4, p. 524, 1978.
2. S. W. Dean, G. D. Grab, *CORROSION/84*, Paper No. 147, National Association of Corrosion Engineers, Houston, Texas, 1984.
3. D. C. Silverman, *Corrosion*, Vol. 40, No. 5, p. 220, 1984.
4. D. C. Silverman, unpublished results presented at the ASTM Electrochemical Workshop, Williamsburg, Virginia, November 1984.
5. M. S. El-Basiouny, S. Haruyama, *Corros. Sci.*, Vol. 16, p. 529, 1976.
6. I. Epelboin, M. Keddam, O. R. Mattos, H. Takenouti, *Corros. Sci.*, Vol. 19, p. 1105, 1979.
7. K. Asami, K. Hashimoto, S. Shimodaira, *Corros. Sci.*, Vol.

- 16, p. 387, 1976.
8. E. A. Lizlovs, A. P. Bond, *J. Electrochem. Soc.*, Vol. 188, No. 1, p. 22, 1971.
  9. B. Alexandré, A. Caprani, J. C. Charbonnier, M. Keddani, Ph. Morel, *Corros. Sci.*, Vol. 21, No. 11, p. 765, 1981.
  10. C. Leygraf, G. Hultquest, I. Olejford, B.-O. Elfstrom, V. M. Knyazheva, A. V. Plaskeyev, Ya. M. Kolotyркиn, *Corros. Sci.*, Vol. 19, p. 343, 1979.
  11. M. Eisenberg, C. W. Tobias, C. R. Wilke, *J. Electrochem. Soc.*, Vol. 101, No. 6, p. 306, 1954.
  12. *Solubilities of Inorganic and Organic Compounds*, H. L. Silcock, Ed., Vol. 3, Part 1, Pergamon Press, Oxford, United Kingdom, p. 452, 1979.
  13. C. R. Wilke, *Chem. Eng. Progr.*, Vol. 45, No. 3, p. 218, 1949.
  14. O. T. Fasulo, *Sulfuric Acid—Use and Handling*, McGraw-Hill Book Co., Inc., New York, New York, 1965.
  15. *International Critical Tables*, Vol. 5, McGraw-Hill Book Co., Inc., New York, New York, 1929.
  16. D. R. Gabe, *J. Appl. Electrochem.*, Vol. 4, p. 91, 1974.
  17. P. A. Mekanjuola, D. R. Gabe, *Surf. Technol.*, Vol. 24, p. 29, 1985.
  18. M. Seo, N. Sato, *Surf. Sci.*, Vol. 86, p. 601, 1979.
  19. V. Mitrovic-Scepanovic, B. MacDougall, M. J. Graham, *Corros. Sci.*, Vol. 24, No. 5, p. 479, 1984.
  20. *Handbook of Physics and Chemistry*, 59th ed., CRC Press, Inc., West Palm Beach, Florida, 1979.

21. I. Cornet, R. Kappesser, *Trans. Inst. Chem. Eng.*, Vol. 47, p. T194, 1969.

### List of Symbols

A	= area (m <sup>2</sup> )
C <sub>B</sub>	= bulk concentration (mol·m <sup>-3</sup> )
C <sub>S</sub>	= surface concentration (mol·m <sup>-3</sup> )
d	= diameter (m)
D	= diffusion coefficient (m <sup>2</sup> ·s <sup>-1</sup> )
F	= Faraday's constant (96,490 coulomb-equivalent <sup>-1</sup> )
i	= CD (coulomb·m <sup>-2</sup> ·s <sup>-1</sup> )
k	= mass transfer coefficient (m·s <sup>-1</sup> )
M	= molecular weight (kg·mol <sup>-1</sup> )
n	= equivalent·mol <sup>-1</sup>
R	= mass transfer rate (mol·m <sup>-2</sup> ·s <sup>-1</sup> )
Re	= Reynolds number ( $\rho v d / \mu$ )
Sc	= Schmidt number ( $\mu / \rho D$ )
Sh	= Sherwood number (kd/D)
t	= time (s)
v	= fluid velocity (m·s <sup>-1</sup> ) (rotation rate = $\omega d/2$ )
w	= weight loss (kg)
$\mu$	= viscosity (poise)
$\rho$	= density (kg·m <sup>-3</sup> )
$\omega$	= rotation rate (rad·s <sup>-1</sup> )